J. Fluid Mech. (2004), *vol.* 519, *pp.* 183–199.
DOI: 10.1017/S0022112004001314 Printed in the United Kingdom

Nonlinear resonant oscillations in closed tubes of variable cross-section

By MICHAEL P. MORTELL[1] AND BRIAN R. SEYMOUR[2]

[1]Department of Applied Mathematics, University College, Cork, Ireland

[2]Department of Mathematics, University of British Columbia, Vancouver, V6T 1Z2 Canada

(Received 27 February 2004 and in revised form 17 July 2004)

An axisymmetric tube with a variable cross-sectional area, closed at both ends, containing a polytropic gas is oscillated parallel to its axis at or near a resonant frequency. The resonant gas oscillations in an equivalent tube of constant cross-section contain shocks. We show how cone, horn and bulb resonators produce shockless periodic outputs. The output consists of a dominant fundamental mode, where its amplitude and detuning are connected by a cubic equation – the amplitude–frequency relation. For the same gas, a cone resonator exhibits a hardening behaviour, while a bulb resonator may exhibit a hardening or softening behaviour. These theoretical results agree qualitatively with available experimental results and are the basis for resonant macrosonic synthesis (RMS).

1. Introduction

This paper is motivated by the experimental results presented in Lawrenson *et al.* (1998). They showed that by appropriately designing the shape of a closed container the resonant oscillations of a gas in the container could reach macrosonic pressures while remaining shockless. This result is in sharp contrast to resonant oscillations in closed uniform cylindrical tubes, where acoustic saturation due to shocks is a feature of the motion, see Betchov (1958), Gorkov (1963), Chester (1964), Seymour & Mortell (1973, 1980) for periodic resonant oscillations, and Cox & Mortell (1983) and Seymour & Mortell (1985) for the evolution of resonant oscillations. Our primary purpose here is to demonstrate theoretically that for resonant cavities shaped like a cone, a horn or a bulb, the nonlinear interaction between the cavity shape and the gas leads to a shockless resonant output. The deliberate shaping of a waveform by designing the shape of the resonator (i.e. the cross-sectional area variation of the containing tube) to give the desired output is the basis for resonant macrosonic synthesis (RMS) (see Lawrenson *et al.* 1998). The significance of RMS is that continuous waveforms can be synthesized to allow a large amount of energy to be added to the wave and extremely high dynamic pressure achieved while avoiding acoustic saturation due to shocks. In this paper, we present the first analytical solutions corresponding to RMS, and compare them with the numerical results of Ilinskii *et al.* (1998) and Chun & Kim (2000).

Nonlinear resonant acoustic oscillations in a straight tube of constant circular cross-section have been the subject of many studies over the last fifty years. The review by Ilgamov *et al.* (1996) gives an extensive list of references. The question naturally arises as to whether specific tube shapes can prevent the formation of shocks, and hence allow a continuous (shockless) harmonic response to a resonant

harmonic input. It has been known since the work of Mortell & Seymour (1972) that small area variations, or 'weak' inhomogeneities, satisfying the conditions of geometrical acoustics, do not prevent shock formation in a medium of finite extent (see also Seymour & Mortell 1975). Keller (1977) investigated the case of pipes with slowly varying cross-section and produced a nonlinear differential-integral equation to describe the signal in the pipe. While this equation has been widely investigated, see for example Ellermeier (1994) or Chester (1994), it suffers from the basic defect of describing only small variations of a straight tube. It is therefore inherently incapable of dealing with shapes such as the cones and bulbs used in the experiments of Lawrenson *et al.* (1998). Chester (1991), by a careful choice of the condition at the centre of a sphere, found continuous periodic oscillations inside a pulsating sphere with a Duffing-like amplitude–frequency response. However, Galiev (1999) points to recent work where an oscillating gas bubble produces a shock wave near the bubble centre. Ellermeier (1994) used a technique similar to that of Chester (1994) to examine the effect of material inhomogeneities on the resonant oscillations of a nonlinear elastic slab. While he produced an equation to describe the relation between the amplitude and frequency of resonant oscillations (i.e. a Duffing-like response), no case of a particular inhomogeneity was solved.

There are two significant numerical investigations of RMS: those of Ilinskii *et al.* (1998) and Chun & Kim (2000). Ilinskii *et al.* (1998) gave a numerical solution for the problem and reproduced qualitatively the amplitude–frequency curves of the experiments of Lawrenson *et al.* (1998). In a subsequent paper, Ilinskii, Lipkens & Zabolotskaya (2001) included the effects of a thermoviscous boundary layer and a simple turbulence model. Chun & Kim (2000) gave numerical solutions of the one-dimensional nonlinear equations for resonant oscillations that explicitly include attenuation terms related to viscosity. They found that the half-cosine-shape tube (similar to a bulb) induced higher compression ratios than other shapes. The analytical study of Ockendon *et al.* (1993) considered geometric variations characterized by different orders of magnitude of the small parameter, and the equations of Chester (1994) and Keller (1977) were recovered. The regime where area variations are large enough to affect the linearized spectrum was also considered briefly, but no explicit solution for any shape like a cone, horn or bulb was attempted. The authors also gave a condition for the applicability of a quasi-one-dimensional model, used here and in Ilinskii *et al.* (1998) and Chun & Kim (2000). Our asymptotic results hold in this region, but we have not so restricted our investigation when comparing with the results of the numerical integrations of Ilinskii *et al.* (1998) and Chun & Kim (2000). Hamilton, Ilinskii & Zabolotskaya (2001) examined the case of a tube with a slowly varying cross-section. However, they were also limited to small variations in cross-sectional area of a cylinder with constant, but arbitrary, cross-section. Again, this has the limitation of not being able to deal with the shapes of interest for RMS. Finally, Mortell & Seymour (2004) have analysed the resonant forced oscillations of a nonlinear elastic panel where the material inhomogeneity has a 'cone-like' structure. The amplitude–frequency curves are explicitly calculated and the dependence on various parameters exhibited.

It is well known that the critical factor in the formation of shock waves in a straight cylindrical tube is the excitation, via nonlinearity, of an infinite number of modes whose frequencies are integer multiples of the fundamental. The modes emerge from linear undamped acoustic theory. Thus, it makes sense to seek resonator shapes leading to eigenvalues of the linear problem that are not integer multiples of the lowest eigenvalue, when the eigenvalues are said to be *incommensurate*. Then we can

expect that shocks will not form and a continuous periodic output, dominated by the lowest eigenmode, will follow. The experimental results of Lawrenson *et al.* (1998) indicate quite clearly that conical, horn and bulb shaped resonators allow shock-free motions. Thus, for these shapes, the linear eigenvalue problem should yield incommensurate eigenvalues. Of course the critical question then is whether we can solve the corresponding two-point boundary-value problem for the eigenfunctions and the eigenvalues. Using a technique introduced by Varley & Seymour (1988), we find a class of resonator shapes, including conical and bulb shapes, for which the acoustic eigenvalue problem can be solved explicitly. Thus, the solution to the nonlinear resonant problem is continuous (shockless) with an amplitude that depends on the detuning from resonance. We use a Duffing-type perturbation expansion to find the amplitude–frequency relation. Mortell & Seymour (2005) is a simple example of this procedure. It should be noted that the procedure given here does not depend on resonator shapes being small deviations from the cylindrical.

2. Formulation and linear theory

We consider the one-dimensional motion of a polytropic gas contained in a tube of arbitrary axisymmetric shape and length L. The tube is closed at both ends and is oscillated along its axis by an external periodic driving force. This is essentially the experimental set-up of Lawrenson *et al.* (1998). It is our objective to reproduce theoretically their experimental amplitude–frequency curves for tubes shaped like cones or bulbs.

Following Ilinskii *et al.* (1998), we use Eulerian coordinates moving with the resonator. If $s(x)$ is the cross-sectional area and $a(t)$ the imposed acceleration of the resonator, the equations of conservation of mass and momentum relating the velocity and density in a polytropic gas are:

$$\frac{\partial(s\rho)}{\partial t} + \frac{\partial}{\partial x}(su\rho) = 0, \tag{1}$$

and

$$\frac{\partial u}{\partial t} + u\frac{\partial u}{\partial x} + \rho^{-1}\frac{\partial p}{\partial x} = -a(t). \tag{2}$$

Pressure and density are measured from their values in a reference state (p_0, ρ_0), so that

$$\frac{p}{p_0} = \left(\frac{\rho}{\rho_0}\right)^{\gamma} = (1+e)^{\gamma} = 1 + \gamma e + \frac{\gamma(\gamma-1)}{4}e^2 + \ldots, \tag{3}$$

where $e(x,t) = \rho/\rho_0 - 1$ is the condensation, and $a_0 = \sqrt{\gamma p_0/\rho_0}$ the associated sound speed. Velocity, pressure and density are non-dimensionalized with respect to $(a_0, \rho_0 a_0^2, \rho_0)$, and (u, p, ρ) are considered as functions of length and time $(Lx, La_0^{-1}t)$. Equation (2) becomes

$$\frac{\partial u}{\partial t} + u\frac{\partial u}{\partial x} + \rho^{\gamma-2}\frac{\partial \rho}{\partial x} = -a(t). \tag{4}$$

For later convenience, we introduce the new variables $e(x,t)$, $f(x,t)$ by

$$f(x,t) = s(x)u(x,t), \quad e(x,t) = \rho(x,t) - 1. \tag{5}$$

Since the resonator is closed at both ends, the boundary conditions are

$$f(0,t) = 0 = f(1,t). \tag{6}$$

To examine the resonance problem we take the applied acceleration as

$$a(t) = \varepsilon^3 \cos\theta, \tag{7}$$

where $\theta = \omega t$ and $0 < \varepsilon \ll 1$.

We seek periodic solutions that have the same period as the external forcing:

$$f\left(x, t + \frac{2\pi}{\omega}\right) = f(x, t), \tag{8}$$

and assume a perturbation expansion of the form:

$$e(x, t) = \varepsilon e_1(x, t) + \varepsilon^2 e_2(x, t) + \varepsilon^3 e_3(x, t) + \ldots, \tag{9}$$

$$f(x, t) = \varepsilon f_1(x, t) + \varepsilon^2 f_2(x, t) + \varepsilon^3 f_3(x, t) + \ldots, \tag{10}$$

where $|e_i|, |f_i| = O(1)$, $i = 1, 2, 3 \ldots$.

Then, at $O(\varepsilon)$, we obtain the linear problem on $0 \leqslant x \leqslant 1$:

$$\frac{\partial f_1}{\partial t} + s(x)\frac{\partial e_1}{\partial x} = 0, \quad s(x)\frac{\partial e_1}{\partial t} + \frac{\partial f_1}{\partial x} = 0, \tag{11}$$

with

$$f_1(0, t) = 0, \quad f_1(1, t) = 0. \tag{12}$$

Eliminating e_1 from (11), $f_1(x, t)$ satisfies

$$\frac{\partial^2 f_1}{\partial t^2} - s(x)\frac{\partial}{\partial x}\left(\frac{1}{s}\frac{\partial f_1}{\partial x}\right) = 0, \tag{13}$$

which is the Webster horn equation (Pierce 1989).

Separating variables:

$$f_1(x, t) = X(x)T(t) \tag{14}$$

leads to the eigenvalue problem on $0 \leqslant x \leqslant 1$:

$$\frac{\mathrm{d}}{\mathrm{d}x}\left(\frac{1}{s(x)}\frac{\mathrm{d}X}{\mathrm{d}x}\right) + \frac{\lambda^2}{s(x)}X = 0, \tag{15}$$

with

$$X(0) = 0, \quad X(1) = 0. \tag{16}$$

Linear equations such as (12) and (13) are standard in problems where material properties vary with position, see Ellermeier (1994). The crux of the matter arises, of course, in solving (12) and (13) analytically for physically interesting area functions $s(x)$. We are not aware of the use of analytical solutions to (12) and (13) that correspond qualitatively to the resonator shapes in the experiments described in Lawrenson *et al.* (1998). Such solutions are, however, implicit in the work of Varley & Seymour (1988), and here we exploit these to solve the acoustic resonance problem in tubes of varying cross-sectional area that correspond to experimental conditions.

3. Nonlinear theory; amplitude-frequency relation

We will assume, *pro tem*, that solutions $f_1(x, t)$ to (14)–(16) are of the form

$$f_1(x, \theta) = A\phi(x)\sin\theta, \tag{17}$$

where A is an arbitrary amplitude. Here, $\phi(x)$ is the eigenfunction determined by (15) and (16) corresponding to the fundamental eigenvalue λ_1, and normalized so that

$$\int_0^1 s^{-1}(x)\phi^2(x)\,\mathrm{d}x = 1, \tag{18}$$

while

$$\theta = \omega t = (\lambda_1 + \varepsilon^2\delta + \ldots)t, \tag{19}$$

where $\varepsilon^2\delta$ measures the detuning.

On using (11) and (17), the corresponding representation for $e_1(x,\theta)$ is

$$e_1(x,\theta) = \frac{A}{\lambda_1 s(x)}\phi'(x)\cos\theta. \tag{20}$$

It should be noted from (19) that we have expanded the frequency, ω, in a Duffing-like expansion about the fundamental frequency $\omega = \lambda_1$. It will emerge at $O(\varepsilon^3)$ that the amplitude A, arbitrary within linear theory, will be connected to the frequency ω through the amplitude–frequency relation.

The equation to determine $f_2(x,\theta)$ now becomes

$$\frac{\partial}{\partial x}\left(\frac{1}{s}\frac{\partial f_2}{\partial x}\right) - \frac{{\lambda_1}^2}{s}\frac{\partial^2 f_2}{\partial\theta^2} = A^2 C_2(x)\sin 2\theta, \tag{21}$$

where

$$C_2(x) = \frac{\lambda_1}{s^2}\left[(\gamma+1)\phi\phi' - 2\frac{s'}{s}\phi^2\right],$$

and

$$f_2(0,\theta) = 0, \quad f_2(1,\theta) = 0. \tag{22}$$

Then, setting

$$f_2(x,\theta) = A^2 B(x)\sin 2\theta, \tag{23}$$

$B(x)$ is determined by

$$\frac{\mathrm{d}}{\mathrm{d}x}\left(\frac{1}{s}\frac{\mathrm{d}B}{\mathrm{d}x}\right) + \frac{(2\lambda_1)^2}{s}B = C_2(x), \tag{24}$$

with

$$B(0) = 0, \quad B(1) = 0. \tag{25}$$

Since $2\lambda_1$ is not an eigenvalue, $B(x)$ exists.

The equation to determine $f_3(x,\theta)$ is of the form

$$\frac{\partial}{\partial x}\left(\frac{1}{s}\frac{\partial f_3}{\partial x}\right) - \frac{{\lambda_1}^2}{s}\frac{\partial^2 f_3}{\partial\theta^2} = C_1(x)\sin\theta + A^3 C_3(x)\sin 3\theta, \tag{26}$$

with

$$f_3(0,\theta) = 0, \quad f_3(1,\theta) = 0, \tag{27}$$

and where

$$C_1(x) = \left[A^3 E_1(x) + A\frac{\delta\phi'}{\lambda_1 s}\right]' + \lambda_1\left[A^3 C_4(x) - 1 - A\frac{\delta\phi}{s}\right]. \tag{28}$$

In (28),

$$C_4(x) = -\frac{1}{2s}\left[\phi\left(\frac{B}{s}\right)' + B\left(\frac{\phi}{s}\right)'\right] + \frac{(\gamma-2)}{s}\left[\lambda_1\left(\phi D - \frac{1}{\lambda_1^2}\phi' D'\right) + \frac{1}{4s}(\phi B' + 4\phi' B)\right] - \frac{(\gamma-2)}{8s^3}\left[\lambda_1\phi^3 - \frac{2s'}{\lambda_1 s}\phi^2\phi'\right] + \frac{(\gamma-2)(\gamma-6)}{8\lambda_1 s^3}\phi(\phi')^2, \tag{29}$$

$$D(x) = \int_0^x \left\{\frac{1}{2s^2}\left[(\gamma-3)\phi\phi' + \frac{s'}{s}\phi^2\right]\right\} \mathrm{d}x, \tag{30}$$

and

$$E_1(x) = -\frac{1}{4\lambda_1 s^2}\left[\left(\phi' B' + 2\lambda_1^2\phi B\right)\right] - \frac{1}{s}(\phi D)' + \frac{1}{8s^3}\left[(2\gamma-3)\phi^2\phi' - \frac{2s'}{s}\phi^3 + \frac{1}{\lambda_1^2}(\phi')^3\right]. \tag{31}$$

Note that, except for the detuning and forcing terms, all terms on the right-hand side of (26) are proportional to A^3. The details of $C_3(x)$ are not required in the rest of the analysis.

Now we let

$$f_3(x,\theta) = P(x)\sin\theta + Q(x)\sin 3\theta. \tag{32}$$

The equation to determine $Q(x)$ is of the form

$$\frac{\mathrm{d}}{\mathrm{d}x}\left(\frac{1}{s}\frac{\mathrm{d}Q}{\mathrm{d}x}\right) + \frac{(3\lambda_1)^2}{s}Q = A^3 C_3(x), \tag{33}$$

with

$$Q(0) = 0, \quad Q(1) = 0. \tag{34}$$

Since $3\lambda_1$ is not an eigenvalue, $Q(x)$ exists with no restriction on A.

$P(x)$ is determined by

$$\frac{\mathrm{d}}{\mathrm{d}x}\left(\frac{1}{s}\frac{\mathrm{d}P}{\mathrm{d}x}\right) + \frac{\lambda_1^2}{s}P = A^3[\lambda_1 C_4(x) + E_1'(x)] - A\lambda_1\delta\left[\frac{\phi}{s} - \lambda_1^{-2}\left(\frac{\phi'}{s}\right)'\right] - \lambda_1, \tag{35}$$

with

$$P(0) = 0, \quad P(1) = 0. \tag{36}$$

Since λ_1 is an eigenvalue, a solution to (35) and (36) exists only if

$$\int_0^1 \left\{A^3[\lambda_1 C_4(x) + E_1'(x)] - A\lambda_1\delta\left[\frac{\phi}{s} - \lambda_1^{-2}\left(\frac{\phi'}{s}\right)'\right] - \lambda_1\right\}\phi(x)\,\mathrm{d}x = 0. \tag{37}$$

This simplifies to

$$\int_0^1 \{A^3[\lambda_1 C_4(x) + E_1'(x)] - \lambda_1\}\phi(x)\,\mathrm{d}x = 2A\lambda_1\delta. \tag{38}$$

Equation (38) is thus the required amplitude–frequency relation that implies that A satisfies the cubic equation

$$NA^3 - 2\delta\lambda_1 A = M, \tag{39}$$

where

$$N = \int_0^1 [\lambda_1 C_4(x) + E_1'(x)]\phi(x)\,\mathrm{d}x, \quad M = \lambda_1 \int_0^1 \phi\,\mathrm{d}x. \tag{40}$$

For a specific area variation $s(x)$, equation (39) will yield an amplitude–frequency curve relating the amplitude A and the detuning δ for the shaking of a closed tube in the neighbourhood of the fundamental resonance.

If the tube is at rest, but the gas is driven by a piston at $x = 1$, the boundary condition (6) is replaced by

$$f(1, t) = \varepsilon^3 \cos\theta. \tag{41}$$

$P(x)$ is now determined by

$$\frac{\mathrm{d}}{\mathrm{d}x}\left(\frac{1}{s}\frac{\mathrm{d}P}{\mathrm{d}x}\right) + \frac{\lambda_1^2}{s}P = A^3[\lambda_1 C_4(x) + E_1'(x)] - A\lambda_1\delta\left[\frac{\phi}{s} - \lambda_1^{-2}\left(\frac{\phi'}{s}\right)'\right], \tag{42}$$

with

$$P(0) = 0, \quad P(1) = 1, \tag{43}$$

where $C_4(x)$ and $E_1(x)$ are given by (29) and (31).

The amplitude–frequency relation is then (39) with N given by (40) and

$$M = \int_0^1 \left[\lambda_1^2\frac{x}{s} + \left(\frac{1}{s}\right)'\right]\phi\,\mathrm{d}x. \tag{44}$$

It remains to implement (39) by specifying $s(x)$ corresponding to the cone, horn or bulb resonators, and solving (15), (16) for the eigenfunction $\phi(x)$.

If $N = 0$ in (39), our expansion yields the linear result, with unbounded amplitude for $\delta = 0$. In this case, we adjust our ansatz and in (7) take the applied acceleration to be $a(t) = \varepsilon^5 \cos\theta$, with the expansion for θ in (19) being $\theta = (\lambda_1 + \varepsilon^4\delta + \ldots)t$. Then, the expansions (9) and (10) yield a quintic equation for A at $O(\varepsilon^5)$.

4. Solution of eigenfunction equations for variable area

To solve the nonlinear acoustic problem (1) to (8), we must first solve the linear equation with variable coefficients of the form (see (11)),

$$\lambda_1^2\frac{\partial^2 g}{\partial\theta^2} - s(x)\frac{\partial}{\partial x}\left(\frac{1}{s}\frac{\partial g}{\partial x}\right) = 0. \tag{45}$$

Varley & Seymour (1988) showed that solutions of (45) can be written in terms of solutions of the equivalent *constant coefficient* equation

$$\lambda_1^2\frac{\partial^2 G}{\partial\theta^2} - \frac{\partial^2 G}{\partial x^2} = 0 \tag{46}$$

by transformations of the form

$$g(x) = R(x)\frac{\partial^2 G}{\partial x^2} + q_1(x)\frac{\partial G}{\partial x} + k_2 G, \tag{47}$$

where $R(x) = \sqrt{s(x)}$ and k_2 is a constant. $s(x)$, $q_1(x)$ are determined by the ordinary differential equations

$$k_2 + \left(\frac{q_1}{s} + \frac{s'}{2s^{3/2}}\right)' = \frac{l_2}{s}, \tag{48}$$

$$l_2 + q_1' = k_2 s, \tag{49}$$

and k_2, l_2 are arbitrary constants. Thus, the solutions $s(x)$ and $q_1(x)$ of (48) and (49) allow the reduction of the variable coefficient equation (45) to the constant coefficient equation (46) through the transformation (47). Accordingly, we can define the shapes $s(x)$ of the resonator for which the simple closed-form solutions of the eigenfunction equation (45) can be found.

The equations (48) and (49) correspond to the case $N=2$ in Varley & Seymour (1988). There, it is shown that the solutions for $R(x)$ and $q_1(x)$ are given by

$$R(x) = \frac{1}{k_2}\frac{\mu_2 z_1 - \mu_1 z_2}{z_2 - z_1}, \tag{50}$$

$$q_1(x) = \frac{\mu_1 - \mu_2}{k_2}\frac{z_1 z_2}{z_2 - z_1}, \tag{51}$$

where z_1, z_2 satisfy the Riccati equation

$$z_n' + z_n^2 = \mu_n \quad (n=1,2), \tag{52}$$

and $k_2 l_2 = \mu_1 \mu_2$. Then, one solution of (52) is

$$z_n(x) = -\sqrt{-\mu_n}\tan[\sqrt{-\mu_n}(x + x_n)], \tag{53}$$

where x_n is an arbitrary constant.

The varying cross-sectional area $s(x) = R^2(x)$ given by (50) and (53) are general enough to generate non-monotonic shapes such as a bulb. For this case, $N=2$, the eigenfunction $\phi_1(x)$ for (15) and (16) is now of the form

$$\phi_1(x) = R(x)F''(x) + q_1(x)F'(x) + k_2 F, \tag{54}$$

with

$$F'' + \lambda^2 F = 0. \tag{55}$$

For the simpler case, $N=1$, the corresponding result is

$$R(x) = -\frac{1}{k_1}z_1, \;\; k_1 l_1 = \mu_1, \tag{56}$$

where

$$\phi_1(x) = R(x)F'(x) - k_1 F. \tag{57}$$

We note that $R(x)$ given by (56) is monotonic and hence corresponds to shapes such as a horn or a cone. A special limit of the $N=1$ case corresponding to the limit $l_1 \to 0$ yields the cone shape:

$$R(x) = 1 + kx. \tag{58}$$

For more details and generalizations of the above, see Varley & Seymour (1988).

5. Cone, horn and bulb resonators

We are now in a position to solve the eigenvalue problem (15) and (16) for a resonator shaped like a cone, a horn and a bulb. For the bulb shape we need the $N=2$ representation for $R(x)$ given by (50); for the horn, $N=1$ and $R(x)$ is given by (56). The cone is a special case of the horn corresponding to $l_1 \to 0$, given by (58).

5.1. *Cone resonator:* $R(x) = (1 + kx)$

A cone is the simplest example of a non-uniform shape for which there is an exact solution to (15) and (16). We let

$$\phi_1(x) = (1 + kx)F' - kF \tag{59}$$

for an arbitrary constant k, where $F(x)$ satisfies (55). Then direct substitution confirms that $\phi_1(x)$ satisfies (15). Conditions (16) yield the eigenvalue equation

$$\tan\lambda = \frac{\lambda k^2}{\lambda^2 + k\lambda^2 + k^2}. \tag{60}$$

It is clear from (60) that for $k \neq 0$ the higher eigenvalues are not integer multiples of the fundamental. For $k = 7$ (similar to the example in Lawrenson *et al.* 1998), the first three eigenvalues are $\lambda_1 = 3.98$ $(= 1.27\pi)$, $\lambda_2 = 6.95$ $(= 2.21\pi)$, $\lambda_3 = 9.95$ $(= 3.17\pi)$, and these are close to those in figure 6 of Ilinskii *et al.* (1998).

The fundamental eigenfunction is given by

$$\phi_1(x) = \chi\left(\lambda_1 k^2 x\cos\lambda_1 x - \left[\lambda_1^2 + kx\lambda_1^2 + k^2\right]\sin\lambda_1 x\right), \tag{61}$$

where $\lambda = \lambda_1$ is the smallest positive eigenvalue of (60) and the constant χ is determined by (18). Since $3\lambda_1$ is not a solution to (60), the term involving $C_3(x)$ in (26) does not resonate and hence the terms in the perturbation expansion at $O(\varepsilon^3)$ are periodic and thus bounded.

We recover the case of a uniform circular cylinder by setting $k = 0$, so that $R(x) \equiv 1$. Then, the positive eigenvalues of (60) are $\lambda_n = n\pi$, and (61) yields $\phi_1(x) = \sqrt{2}\sin n\pi x$. Now, the higher eigenvalues are integer multiples of the fundamental eigenvalue, resonance in the higher modes cannot be avoided and shocks occur (see Chester 1964; Seymour & Mortell 1980).

5.2. *Horn resonator:* $R(x) = \sqrt{|a/b|}\tan(\sqrt{|ab|}(x + x_0))$

Curved cone-like resonators can be described by cross-sections of the form

$$s(x) = \left|\frac{a}{b}\right|\tan^2(\sqrt{|ab|}(x + x_0)). \tag{62}$$

The results of Varley & Seymour (1988) for the case $N = 1$ imply that, if $s(x)$ is given by (62), then

$$\phi_1(x) = R(x)F' + aF \tag{63}$$

is a solution of (15) for arbitrary constants $a(< 0)$, $b(> 0)$ and x_0, when $F(x)$ satisfies (55). Alternatively, if $\phi_1(x)$ is given by (63) and

$$\frac{1}{s}\phi_1' = \frac{1}{\sqrt{s}}E' + bE \tag{64}$$

with

$$F' = E, \quad E' = -\lambda^2 F, \tag{65}$$

then ϕ_1 is a solution to (15), provided $s(x)$ satisfies

$$\frac{s'}{2\sqrt{s}} + a - bs = 0 \tag{66}$$

which has (62) as one solution.

The boundary conditions (16) yield the eigenvalue equation

$$\tan\lambda = \frac{\lambda(\beta - \alpha)}{\lambda^2 + \alpha\beta}, \tag{67}$$

where

$$\alpha = \frac{a}{R(0)}, \quad \beta = \frac{a}{R(1)}. \tag{68}$$

Again, the eigenvalues are incommensurate, i.e. the higher modes are not integer multiples of the fundamental. The first three eigenvalues for $(\alpha, \beta) = (-0.66, -0.083)$ are $\lambda_1 = 3.31$ $(= 1.05\pi)$, $\lambda_2 = 6.37$ $(= 2.03\pi)$, $\lambda_3 = 9.48$ $(= 3.017\pi)$. The eigenfunction $\phi_1(x)$ is normalized using the condition (18).

We note that Mortell & Seymour (2004) have examined the shockless resonant vibrations of a nonlinear elastic panel with an inhomogeneity given by (62).

5.3. *Bulb resonator:* $R(x) = (\mu_2 z_1 - \mu_1 z_2)/[(z_2 - z_1)k_2]$

Bulb-like resonators are described by cross-sections of the form (50) where $z_1(x)$, $z_2(x)$ are given by (52) and (53). The form of the eigenfunction is then given by (54) and (55), and the eigenfunction is normalized by (18).

The boundary conditions (16) yield the eigenvalue equation

$$\tan\lambda = \frac{\lambda(\lambda^2(q_1R_0 - R_1q_0) - q_1k_2 + k_2q_0)}{(\lambda^4R_1R_0 - \lambda^2(R_1k_2 - q_1q_0 + k_2R_0) + k_2^2)}, \tag{69}$$

where $R_0 = R(0)$, $R_1 = R(1)$, $q_0 = q_1(0)$ and $q_1 = q_1(1)$. The first three eigenvalues are given by $\lambda_1 = 4.43$ $(= 1.41\pi)$, $\lambda_2 = 6.96$ $(= 2.22\pi)$, $\lambda_3 = 9.87$ $(= 3.14\pi)$ when $\mu_1 = -9$, $\mu_2 = -3$, $k_2 = 9.4$, $x_1 = -1.65$, $x_2 = 2$. We note that λ_2 and λ_3 are close to those in figure 12(*a*) in Ilinskii *et al.* (1998) for a bulb with a flare.

6. Results and comparison with experiments

Here, we present results for shapes and amplitudes that are qualitatively similar to those used in the experiments of Lawrenson *et al.* (1998). The values of $\varepsilon = 0.05$, 0.08 and 0.1 are similar to the values in the experiments of Lawrenson *et al.* (1998). The figures illustrate typical shapes for cone, horn and bulb resonators. The corresponding theoretical response curves are compared with the experimental and numerical results where they are available in figures 3–5. In all cases here $\gamma = 1.13$, which corresponds approximately to the gases used in the experiments of Lawrenson *et al.* (1998).

The graphs of the response curves of p_1/p_0 represent the ratio of the amplitude of the pressure signal in the fundamental mode to the ambient pressure at the small end of the resonator, $x = 0$. They are calculated from (3), (5) and (20) by

$$\left|\frac{p_1}{p_0}\right| = \frac{A\gamma\varepsilon\phi_1'(0)}{\lambda_1 s(0)}. \tag{70}$$

The compression ratio at $x = 0$ is then found from:

$$\frac{p_{\max}}{p_{\min}} = \frac{1 + |\gamma(\varepsilon A/\lambda_1 s(0))\,\phi'(0)|}{1 - |\gamma(\varepsilon A/\lambda_1 s(0))\,\phi'(0)|}. \tag{71}$$

Hence, a value of $|p_1/p_0|$ around 0.5 will produce a compression ratio of 3.

The numerical investigation reported in Ilinskii *et al.* (1998) has several authors in common with the experimental paper of Lawrenson *et al.* (1998). While the former state that 'qualitatively, the (numerical) model describes all phenomena observed in the experiments: resonance frequency shift, hysteresis and waveform distortion', the only reported quantitative comparison with experiment is for the wave shape for a conical resonator, see their figure 14 and table 1. The reference point for Bednarik & Cervenka (2000) is the numerical simulations of Ilinskii *et al.* (1998), while Chun & Kim (2000) provide only numerical solutions. Hamilton *et al.* (2001) compare their theory with finite-difference solutions of the complete nonlinear equations for one-dimensional motion in a resonator of arbitrary shape, and conclude that the analytical

results are in reasonable agreement with the numerical results. Ockendon *et al.* (1993) neglect dissipation and have no comparison with experiments.

Because of a lack of experimental input data, a detailed quantitative comparison of the experimental results of Lawrenson *et al.* (1998) with the theoretical predictions given here is not possible. However, qualitatively the simple model given here yields the basic observations of the experiments: the shift in the resonant frequency, hysteresis and waveform distortion from higher harmonics. The cone and horn resonators exhibit a nonlinear hardening behaviour, while the bulb resonator may exhibit a hardening or softening behaviour for the same gas. As remarked in Lawrenson *et al.* (1998), 'if the properties of the gas in the cavities were the primary factor influencing nonlinear behaviour we would expect to see similar frequency response curves.' We have found that for all three cases (cone, horn and bulb), the amplitude response curve is multivalued and strong hysteresis is present. The experiments in Lawrenson *et al.* (1998) and the numerical solutions in Ilinskii *et al.* (1998) show that hysteresis for the cone and bulb occurs only for sufficiently large driver amplitudes. Ilinskii *et al.* (1998) include energy dissipation in their model, and choose the value of a dimensionless attenuation coefficient to match the experimental Q-factor. Subsequently, the effects of the thermoviscous boundary layer and a simple turbulence model were included in Ilinskii *et al.* (2001). We, on the other hand, focus solely on the interaction between the gas nonlinearity and the resonant cavity shape with no form of dissipation included, so there is no doubt as to the fundamental mechanism involved. It is found by Ilinskii *et al.* (1998) that for a bulb with a flare, a very pronounced hysteresis is apparent (see figure 13), and we note that the second and third eigenvalues for our bulb resonator closely match those in Ilinskii's flared bulb and strong hysteresis is predicted.

Our results, including qualitative comparisons with the experiments of Lawrenson *et al.* (1998) and the numerical simulations of Ilinskii *et al.* (1998) and Chun & Kim (2000), are illustrated in figures 1–7. The general forms of the three shapes (cone, horn and bulb) used in the analytical model are shown in figure 1. We choose the parameter $k = 7$ in (58), corresponding to the shape used by Lawrenson *et al.* (1998), and in figure 2 compare our theoretical results with experimental and numerical results. There is good qualitative agreement with Lawrenson *et al.* (1998), Ilinskii *et al.* (1998) and Chun & Kim (2000). Similar comparisons are made in figure 3 for the response curves for a bulb resonator with parameters chosen as: $\mu_1 = -9$, $\mu_2 = -3$, $k_2 = 9.4$, $x_1 = -1.65$, $x_2 = 2$. Again, the qualitative agreement with the experimental and numerical results is clear. In particular, the response curve exhibits a softening behaviour, in contrast to the cone response of figure 2. Figure 4 exhibits the response curves for several horn shapes with increasing values of $R(1) = 2.45, 4.57$ and 8.0. All give hardening responses: there are no experimental or numerical results available for comparison.

Chun & Kim (2000) give a numerical simulation for what they describe as a half-cosine shaped tube. In figure 5, we model the half-cosine shape by scaling the bulb shape of figure 1 by a factor of $W = 0.69$, that is, stretching the bulb shape for $0 \leqslant x \leqslant 0.69$ over $0 \leqslant x \leqslant 1$; $W = 1$ gives the original shape. There is qualitative agreement with Chun & Kim (2000).

A measure of the commercial viability of RMS is the maximum compression ratio, defined by (71). Commercial air compressors must achieve a pressure ratio of between 3 and 13. Lawrenson *et al.* (1998) have reported experimentally produced values of 12 for a cone and 17 for a horn cone, though no numerical simulations have produced ratios as high as these. For example, Ilinskii *et al.* (1998) report a ratio of 6.4 for a cone with an applied dimensionless acceleration of 5×10^{-4}; they report no results for

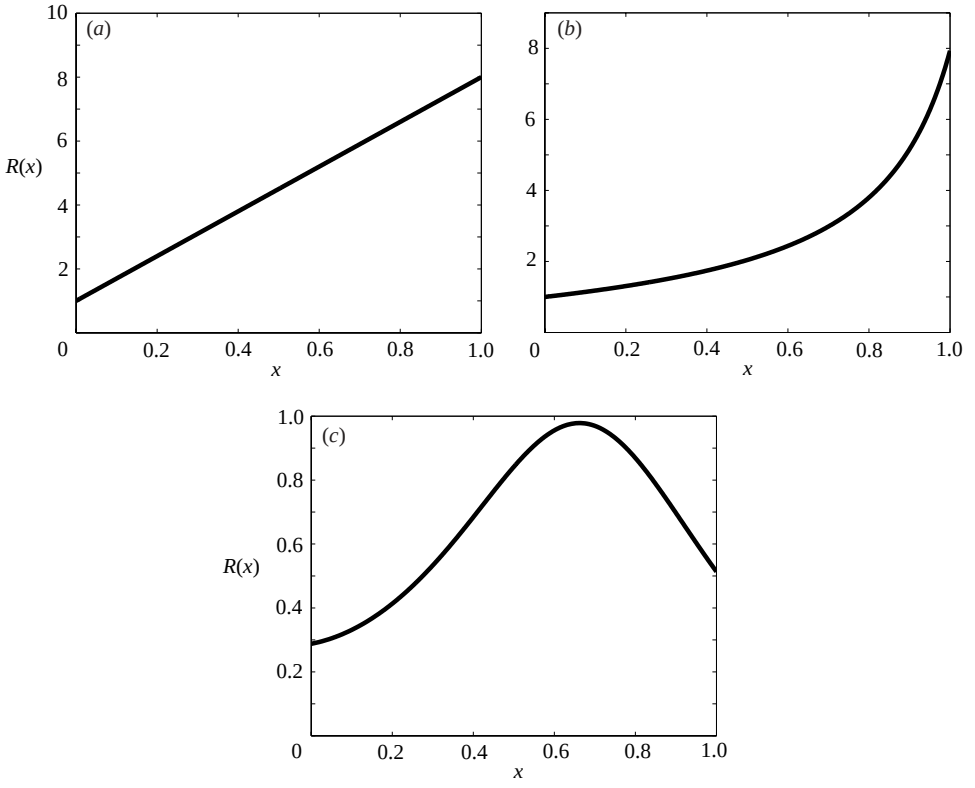

FIGURE 1. Shapes used in analytical model. (*a*) Cone shape. (*b*) Large horn shape. (*c*) Bulb shape.

a bulb or horn cone. Chun & Kim (2000) report a pressure ratio of 3.1 for a cone and 6.5 for their half-cosine shaped tube with an input acceleration of $300\,\mathrm{m\,s^{-2}}$. Here, we find a compression ratio of 4.0 for a cone and 5.0 for a bulb when using $\varepsilon = 0.136$, corresponding to $300\,\mathrm{m\,s^{-2}}$. Qualitatively, our results are more in line with those of Chun & Kim (2000) than Ilinskii *et al.* (1998). The values given by our analytical results lie within the commercial range.

The cubic amplitude–frequency relation (39) results from the ansatz that an applied acceleration at $O(\varepsilon^3)$ yields an output of $O(\varepsilon)$. If, for a specific value of the parameters, $N = 0$ in (39), the expansion produces an unbounded response at $\delta = 0$. However, if now the ansatz in (7) is changed to $a(t) = \varepsilon^5 \cos\theta$, then the perturbation scheme yields a quintic equation for the amplitude A at fifth order, again with an output of $O(\varepsilon)$. We have, of course, neglected all dissipative effects, but in our non-dissipative theory, the maximum amplitude of the peak output is achieved when $N \sim 0$ in (39). By varying W we find that this occurs for $W \sim 0.759$: the corresponding bulb shape is illustrated in figure 6. When W changes from 0.75907 to 0.75908, the response curve changes from hardening to softening as N passes through a zero. The amplification has increased by an order of magnitude around the fundamental resonant frequency. It may be that in an experiment this effect is masked by dissipation, but in designing a resonator for maximum amplitude, choosing a shape for which $N \sim 0$ may well be optimal. This possibility is illustrated in figure 6(*d*), where a compression ratio in excess of 20 is achieved.

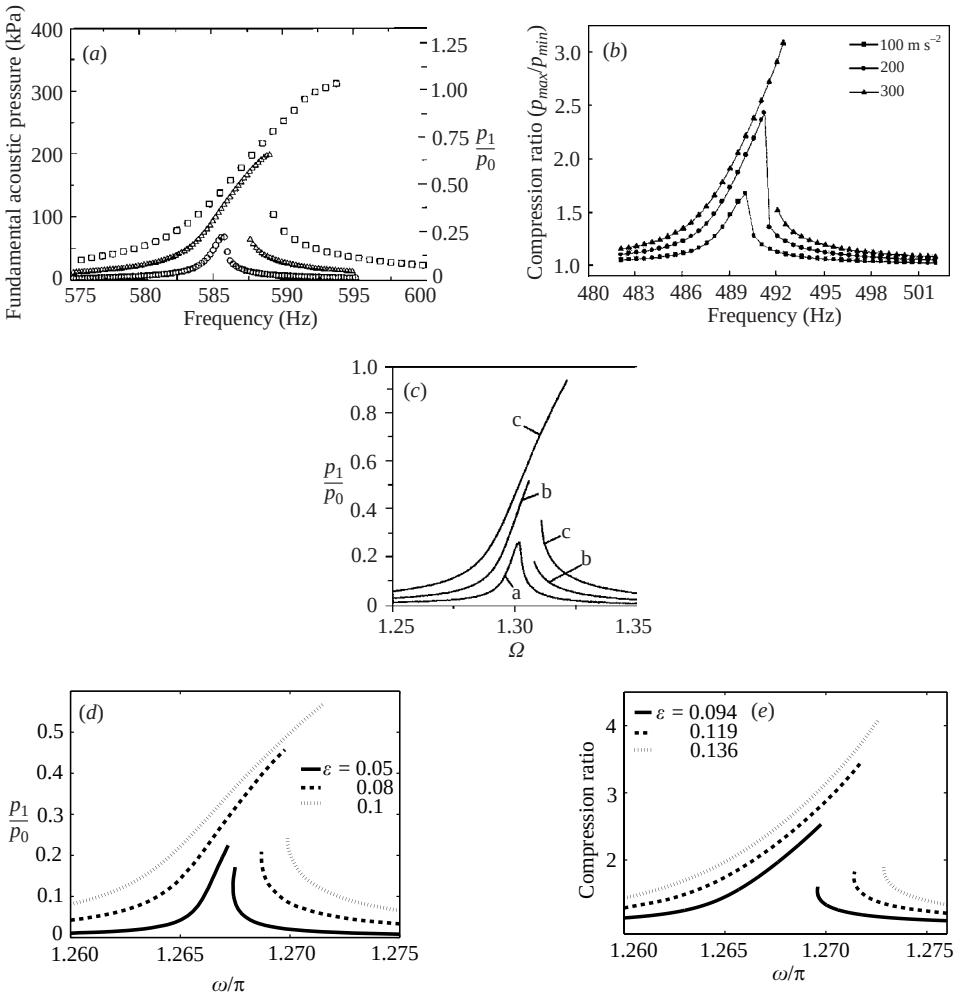

FIGURE 2. Comparison of cone response curves. (*a*) Experimental frequency response curves at three (not identified) drive amplitudes at the small end of a cone resonator filled with R-134a. This is figure 13 in Lawrenson *et al.* (1998). (*b*) Compression ratio as a function of frequency, calculated numerically for three drive accelerations. This is figure 4(*a*) in Chun & Kim (2000). (*c*) Frequency response of the fundamental pressure wave in a conical resonator calculated numerically for non-dimensional drive accelerations 10^{-4}, 2.5×10^{-4} and 5×10^{-4}. This is figure 8 in Ilinskii *et al.* (1998), with the same geometry as in figure 2(*a*) above. (*d*) Theoretical frequency response of the fundamental pressure wave in a conical resonator calculated from equation (70) for drive accelerations corresponding to figure 8 in Ilinskii *et al.* (1998), with the same geometry as in figure 2(*a*) above. (*e*) Theoretical compression ratio (p_{max}/p_{min}) as a function of frequency for a cone resonator, calculated from equation (71), for the three drive accelerations corresponding to figure 4(*a*) in Chun & Kim (2000), reproduced as figure 2(*b*) above.

The amplification is reduced considerably for higher modes. Figure 7 shows the eigenfunction and response curve for a bulb with $W = 0.759$ that is excited close to the second harmonic, $\omega = 2.13\pi$. In contrast to the fundamental mode, $N = 320$ and the response has a relatively small amplitude and is hardening.

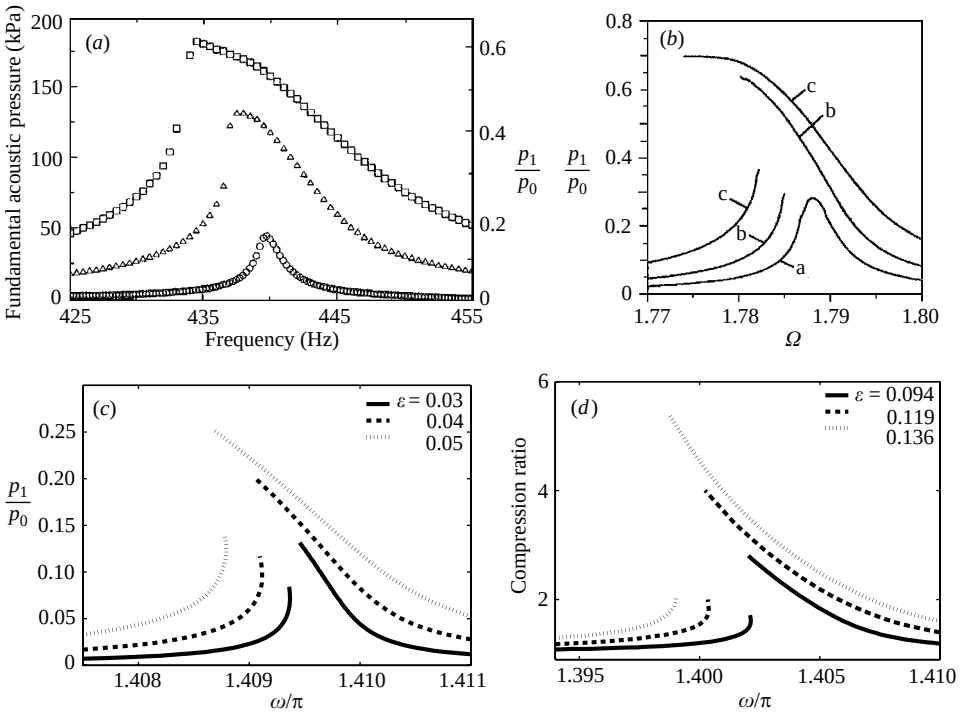

FIGURE 3. Comparison of bulb response curves. (*a*) Experimental frequency response curves at three (not identified) drive amplitudes at the small end of a bulb resonator filled with R-134a. This is figure 14 in Lawrenson *et al.* (1998), with a bulb shape given by their equation (5). (*b*) Frequency response of the fundamental pressure wave in a bulb resonator calculated numerically for non-dimensional drive accelerations 0.25×10^{-4}, 0.5×10^{-4} and 10^{-4}. This is figure 13 in Ilinskii *et al.* (1998); no equation for the bulb is given. (*c*) Theoretical frequency response of the fundamental pressure wave in a bulb resonator, calculated from equation (70), for drive accelerations corresponding to figure 13 in Ilinskii *et al.* (1998). (*d*) Theoretical compression ratio (p_{max}/p_{min}) as a function of frequency for a bulb resonator, calculated from equation (71), corresponding to the three drive accelerations in figure 4(*a*) of Chun & Kim (2000).

Hamilton *et al.* (2001) found analytically for a slowly varying 'cylindrical' tube that if $2\lambda_1 > \lambda_2$ there was a hardening response curve, while if $2\lambda_1 < \lambda_2$ the response curve was softening. This is clearly not the case for the bulb resonator in figure 3 where $\lambda_1 = 1.41\pi$ and $\lambda_2 = 2.22\pi$.

We have examined the effect of the shape of a closed resonant cavity on the nonlinear resonant oscillations of a lossless perfect gas contained within it. In contrast to a circular cylinder, for resonant cavities shaped like a cone, a horn or a bulb, unshocked resonant motions are possible for extremely high overpressures and acoustic saturation is avoided. This is the basis for resonant macrosonic synthesis (RMS). We conclude that a given gas can have a hardening or softening response curve depending on the shape of the container. Different bulb shaped containers can yield a hardening or softening response. Further, this hardening or softening response can depend on the mode of the oscillation. The combination of frequency and bulb shape that yields $N \sim 0$ gives particularly large response amplitudes. The latter three observations have not been reported in experiments.

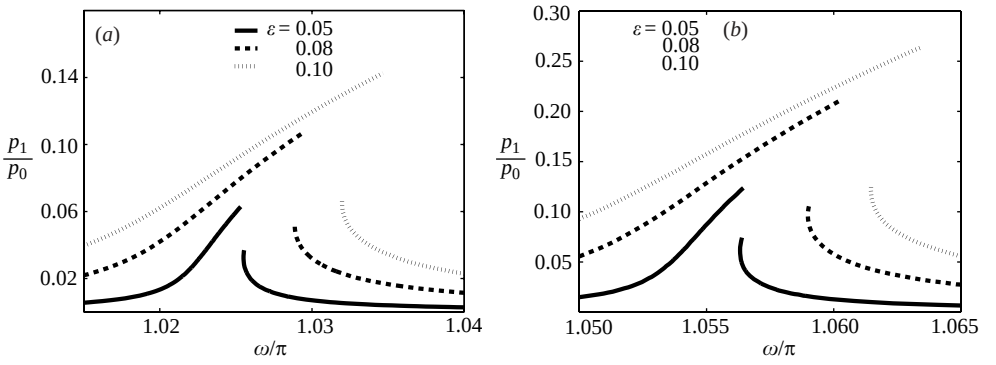

FIGURE 4. Horn response curves. (*a*) Theoretical frequency response of the fundamental pressure wave in a horn resonator with (*a*) small aspect ratio of 2.45, and (*b*) with large aspect ratio of 8, calculated from equation (70).

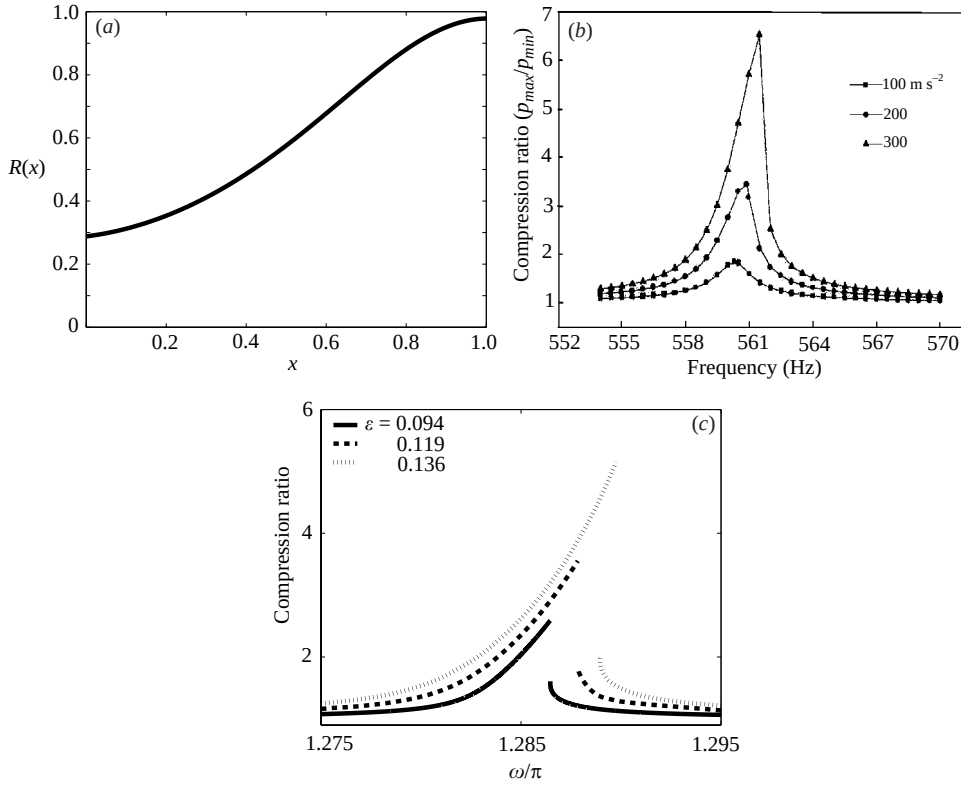

FIGURE 5. Half cosine curves. (*a*) The half-cosine shape, approximated by equation (50) and similar to figure 1(*c*) in Chun & Kim (2000). (*b*) Compression ratio as a function of frequency, calculated numerically for three drive accelerations. This is figure 5(*a*) in Chun & Kim (2000). (*c*) Theoretical compression ratio (p_{max}/p_{min}) as a function of frequency for a half-cosine resonator, calculated from equations (50) and (71), for the three drive accelerations corresponding to figure 5(*a*) in Chun & Kim (2000), reproduced as figure 5(*b*) above.

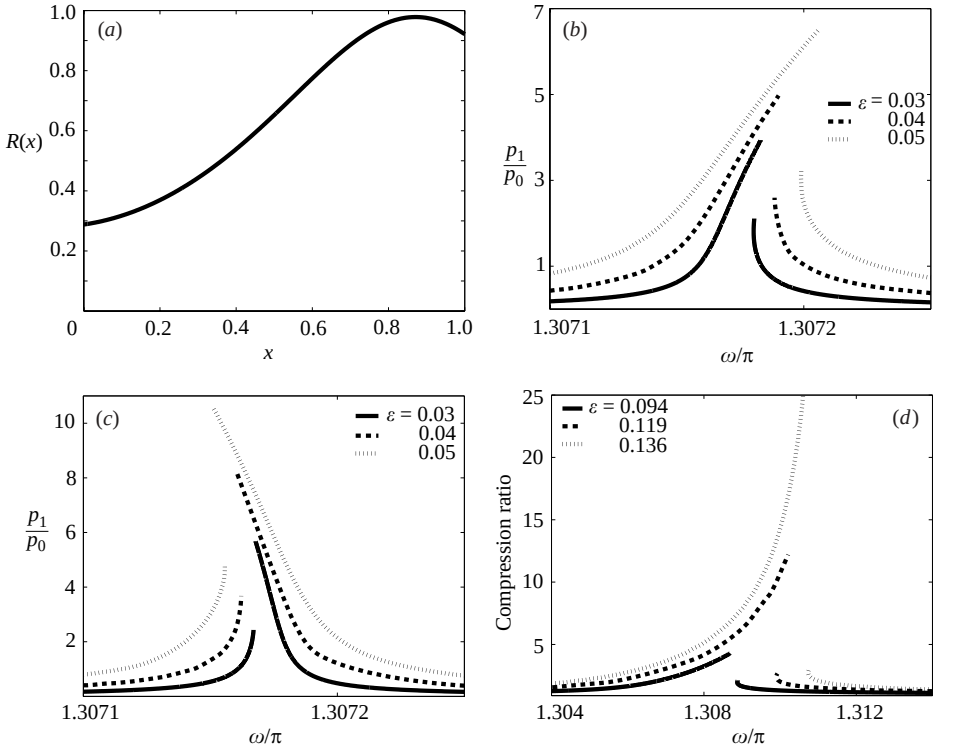

FIGURE 6. Marginal response curves. (*a*) Bulb resonator shape with $W = 0.759$ that produces the maximum compression ratio. (*b*) Theoretical frequency response of the fundamental pressure wave in a bulb resonator with $W = 0.75907$. (*c*) Theoretical frequency response of the fundamental pressure wave in a bulb resonator with $W = 0.75908$. (*d*) Theoretical compression ratio (p_{max}/p_{min}) as a function of frequency for a half-cosine resonator with $W = 0.75907$, calculated from equations (50) and (71), for the three drive accelerations corresponding to figure 5(*a*) in Chun & Kim (2000).

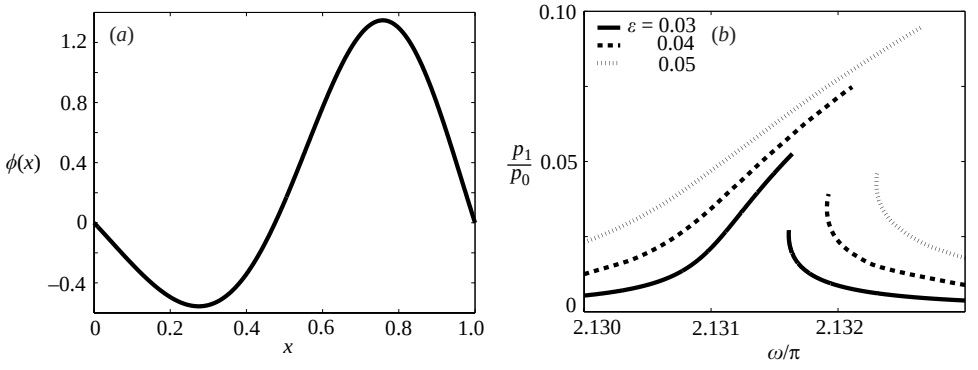

FIGURE 7. Second harmonic response. (*a*) Theoretical eigenfunction for the second harmonic in a bulb resonator with $W = 0.75907$. (*b*) Theoretical frequency response of the second harmonic pressure wave in a bulb resonator with $W = 0.75907$.

The research reported in this paper was supported in part by the Natural Sciences and Engineering Research Council of Canada under grant A9117. We wish to thank Dr E. A. Cox who suggested we look at the problem.

REFERENCES

Bednarik, M. & Cervenka, M. 2000 Nonlinear waves in resonators. In *Nonlinear Acoustics at the Turn of the Millennium*, ISWA 15 (ed. W. Lauterborn & T. Kurz), pp. 163–168.

Betchov, R. 1958 Nonlinear oscillations of a column of gas. *Phys. Fluids* **1**, 205–212.

Chester, W. 1964 Resonant oscillations in a closed tube. *J. Fluid Mech.* **18**, 44–64.

Chester, W. 1994 Nonlinear resonant oscillations of a gas in a tube of varying cross-section. *Proc. R. Soc. Lond.* A **444**, 591–604.

Chester, W. 1991 Acoustic resonance in spherically symmetric waves. *Proc. R. Soc. Lond.* A **434**, 459–463.

Chun, Y.-D. & Kim, Y.-H. 2000 Numerical analysis for nonlinear resonant oscillations of gas in axisymmetric closed tubes. *J. Acoust. Soc. Am.* **108**, 2765–2774.

Cox, E. A. & Mortell, M. P. 1983 The evolution of resonant oscillations in a closed tube. *Z. Angew. Math. Phys.* **34**, 845–866.

Ellermeier, W. 1994 Resonant wave motion in a nonhomogeneous system. *Z. Angew. Math. Phys.* **45**, 275–286.

Galiev, S. U. 1999 Passing through resonance of spherical waves. *Phys. Lett.* A **260,** 225–233.

Gorkov, A. P. 1963 Nonlinear acoustic oscillations of a column of gas in a closed tube. *Inzhenerno-fizicheski jurnal* **3**, 246–250.

Hamilton, M. F., Ilinskii Y. A. & Zabolotskaya, E. A. 2001 Linear and nonlinear frequency shifts in acoustic resonators with varying cross sections. *J. Acoust. Soc. Am.* **110**, 109–118.

Ilgamov, M. A., Zaripov, R. G., Galiullin, R. G. & Repin, V. R. 1996 Nonlinear acoustic oscillations of a column of gas in a tube. *Appl. Mech. Rev.* **49**, 137–154.

Ilinskii, Y. A., Lipkens, B., Lucas, T. S. & Van Doren, T. W. 1998 Nonlinear standing waves in an acoustic resonator. *J. Acoust. Soc. Am.* **104**, 2664–2674.

Ilinskii, Y. A., Lipkens, B. & Zabolotskaya, E. A. 2001 Energy losses in an acoustic resonator. *J. Acoust. Soc. Am.* **109**, 1859–1870.

Keller, J. J. 1977 Nonlinear acoustic resonances in shock tubes with varying cross-sectional area. *Z. angew. Math. Phys.* **28**, 107–122.

Lawrenson, C. C., Lipkens, B., Lucas, T. S., Perkins, D. K. & Van Doren, T. W. 1998 Measurements of macrosonic standing waves in oscillating closed cavities. *J. Acoust. Soc. Am.* **104**, 623–636.

Mortell, M. P. & Seymour, B. R. 1972 Pulse propagation in a nonlinear viscoelastic rod of finite length. *SIAM J. Appl. Maths* **22**, 209–224.

Mortell, M. P. & Seymour, B. R. 2005 Finite amplitude, shockless, resonant vibrations of an inhomogeneous elastic panel. *J. Maths & Mech. Solids* (to appear).

Ockendon, H., Ockendon, J. R., Peake, M. R. & Chester, W. 1993 Geometrical effects in resonant gas oscillations. *J. Fluid Mech.* **257**, 201–217.

Pierce, A. D. 1989 *Acoustics.* Acoustical Society of America, NY.

Seymour, B. R. & Mortell, M. P. 1973 Resonant acoustic oscillations with damping: small rate theory. *J. Fluid Mech.* **58**, 353–374.

Seymour, B. R. & Mortell, M. P. 1975 Nonlinear geometrical acoustics. *Mech. Today* **2**, 251–312.

Seymour, B. R. & Mortell, M. P. 1980 A finite rate theory of resonance in a closed tube: discontinuous solutions of a functional equation. *J. Fluid Mech.* **99**, 365–382.

Seymour, B. R. & Mortell, M. P. 1985 The evolution of a finite rate periodic oscillation. *Wave Motion* **7**, 399–409.

Varley, E. & Seymour, B. R. 1988 A method for obtaining exact solutions to partial differential equations with variable coefficients. *Stud. Appl. Maths* **78**, 183–225.